International Journal of Pharmaceutics 398 (2010) 190–203

Contents lists available at ScienceDirect

International Journal of Pharmaceutics

journal homepage: www.elsevier.com/locate/ijpharm

Pharmaceutical Nanotechnology

Transferrin mediated solid lipid nanoparticles containing curcumin: Enhanced *in vitro* anticancer activity by induction of apoptosis

Rohit S. Mulik[a,c,d], Jukka Mönkkönen[c], Risto O. Juvonen[d], Kakasaheb R. Mahadik[a], Anant R. Paradkar[b,*]

[a] *Department of Pharmaceutics, Poona College of Pharmacy, Bharati Vidyapeeth University, Erandwane, Pune 411038, India*
[b] *Institute of Pharmaceutical Innovation, University of Bradford, Bradford BD7 1DP, UK*
[c] *Department of Pharmaceutics, University of Kuopio, P.O. Box 1627, FIN-70211 Kuopio, Finland*
[d] *Department of Pharmacology and Toxicology, University of Kuopio, P.O. Box 1627, FIN-70211 Kuopio, Finland*

ARTICLE INFO

Article history:
Received 28 March 2010
Received in revised form 10 July 2010
Accepted 13 July 2010
Available online 22 July 2010

Keywords:
Apoptosis
Curcumin
Cytotoxicity
Breast cancer
Flow cytometry

ABSTRACT

Photodegradation and low bioavailability are major hurdles for the therapeutic use of curcumin. Aim of the present study was to formulate transferrin-mediated solid lipid nanoparticles (Tf-C-SLN) to increase photostability, and enhance its anticancer activity against MCF-7 breast cancer cells. Tf-C-SLN were prepared by homogenization method and characterized by size, zeta potential, entrapment efficiency and stability, transmission electron microscopy (TEM), X-ray diffraction (XRD) and *in vitro* release study. Microplate analysis and flow cytometry techniques were used for cytotoxicity and apoptosis study. The physical characterization showed the suitability of method of preparation. TEM and XRD study revealed the spherical nature and entrapment of curcumin in amorphous form, respectively. The cytotoxicity, ROS and cell uptake was found to be increased considerably with Tf-C-SLN compared to curcumin solubilized surfactant solution (CSSS) and curcumin-loaded SLN (C-SLN) suggesting the targeting effect. AnnexinV-FITC/PI double staining, DNA analysis and reduced mitochondrial potential confirmed the apoptosis. The flow cytometric studies revealed that the anticancer activity of curcumin is enhanced with Tf-C-SLN compared to CSSS and C-SLN, and apoptosis is the mechanism underlying the cytotoxicity. The present study indicated the potential of Tf-C-SLN in enhancing the anticancer effect of curcumin in breast cancer cells *in vitro*.

1. Introduction

Curcumin is a naturally occurring phytoconstituent of widely used spice, turmeric (*Curcuma longa* Linn) from India, China and South East Asia. It has very broad spectrum of biological activities such as, anti-inflammatory, antioxidant, antimicrobial, wound healing, and anticarcinogenic (Aggarwal et al., 2005a,b; Aggarwal and Harikumar, 2009; Anand et al., 2008; Chattopadhyay et al., 2004). Various studies in the past few years on curcumin corroborate that it has a strong potential to inhibit the growth of various cancer cells from different origins like skin, prostate, ovarian, colon, breast, brain, blood, liver and pancreas (Aggarwal et al., 2005a,b; Aggarwal and Harikumar, 2009; Anand et al., 2008).

Anticancer potential of curcumin against breast (Ramachandran et al., 2002), prostate (Dorai et al., 2001), colon (Aggarwal et al., 2003a,b) and stomach (Azuine and Bhide, 1992) cancer have been demonstrated in recent years. Although the exact mechanism of curcumin anticancer effect is yet not fully understood, several mechanisms have been proposed (Aggarwal et al., 2003a,b). Anticancer activity often involves modulation of signal transduction pathways, resulting in alterations in gene expression, cell cycle inhibition or apoptosis (Aggarwal et al., 2003a,b; Thangapazham et al., 2006; Joe et al., 2004). Apoptosis is a mode of cell death used by multicellular organisms to irradicate cells in diverse physiological and pathological settings. Recent studies have demonstrated that cell cycle inhibition and induction of apoptosis are the main mechanisms for anticancer effects of curcumin (Joe et al., 2004). The induction of apoptosis by curcumin has been shown to be via generation of reactive oxygen species (Buttke and Sandstrom, 1994; Jacobson, 1996; Christine et al., 2004), and inhibition of NFkB (Aggarwal et al., 2005a,b; Singh and Aggarwal, 1995).

Various type of receptors such as, lipoproteins, folate, different peptide receptors, growth factor receptors, and transferrin overexpress on the surface of malignant tissues compared to normal tissues (Hussain, 2000). Transferrin receptor (Tf receptor) is the ubiquitous cell surface glycoprotein related to cell proliferation and is overexpressed in malignant tissues compared to normal tissues because of the higher iron demand of malignant cells for the fast growth and division (Qian et al., 2002; Widera et al., 2003). Hence,

* Corresponding author. Tel.: +44 1274 233900.
E-mail addresses: A.Paradkar1@Bradford.ac.uk, arparadkar@rediffmail.com (A.R. Paradkar).

0378-5173/$ – see front matter.
doi:10.1016/j.ijpharm.2010.07.021

transferrin mediated drug and gene delivery systems have been developed and studied in the past few years for the tumor specific targeting *in vitro* and *in vivo*. For example, transferrin conjugated PLGA nanoparticles containing paclitaxel for enhanced antiproliferative activity (Sahoo and Labhasetwar, 2005), transferrin–PEG liposomes for intracellular delivery and targeting to solid tumors (Maruyama et al., 2004), transferrin conjugated gold nanoparticles for cancer cell imaging and therapy (Li et al., 2009), transferrin conjugated PEG–albumin nanoparticles for brain targeting (Ulbrich et al., 2009), transferrin receptor-targeted lipid nanoparticles for delivery of an antisense oligodeoxyribonucleotide against Bcl-2 (Yang et al., 2009), Recently, silk fibroin-derived curcumin nanoparticles for breast cancer therapy have been reported (Gupta et al., 2009) but, only cytotoxicity and uptake study has been carried out. Hence, study of probable mechanisms of anticancer activity and therapeutic effectiveness of curcumin encapsulated nanoparticles against breast cancer is still unexplored. Because of the low bioavailability, short half life and photo degradation of curcumin we decided to formulate a transferrin mediated nanoparticulate system which can effectively increase the therapeutic potential of curcumin by reducing these drawbacks.

Overexpression of Tf receptor on the surface of MCF-7 cells is well documented (Vandewalle et al., 1985). The main objective of the present study was to formulate stable transferrin conjugated solid lipid nanoparticles containing curcumin for the targeted cellular delivery to breast cancer cells and evaluate its enhanced anticancer effect. The distinct advantages of prepared formulation are biodegradable and biocompatible delivery system, sustained release of encapsulated curcumin, and, hence, increased therapeutic efficacy. Since, both transferrin (Tf) (Wang et al., 2000; Lemieux and Page, 1994) and curcumin (Chearwae et al., 2006, 2004) are capable of inhibiting p-glycoprotein efflux, bypass of membrane associated efflux transporters could lead to increased cellular uptake and retention of the drug.

2. Materials and methods

2.1. Materials

Hydrogenated soya phosphatidylcholine (HSPC), distearoyl phosphatidyl ethanolamine (DSPE), cholesterol (Chol) were purchased from Lipoid. Triolein was purchased from Sigma Aldrich, USA. Transferrin (Human, low endotoxin) was purchased from Calbiochem, USA. Curcumin was a kind gift from Indsaaf Inc., Batala, India. 1-Ethyl-3-[3-dimethylaminopropyl] carbodiimide hydrochloride (EDC) and coomassie brilliant blue G dye were purchased from Himedia, Mumbai, India. AnnexinV-FITC and propidium iodide were purchased from Biolegend Europe BV, Netherlands. 2′,7′-dichlorodihydrofluorescein diacetate (H2DCF-DA), tetramethyl rhodamine methyl ester (TMRM) were purchased from Sigma Aldrich, Germany. Growth medium RPMI 1640 was purchased from BioWhittaker Inc. (Lonza, Belgium). 3-(4,5-dimethylthiazol-2-yl)-2,5-diphenyl tetrazolium bromide (MTT) was purchased from Sigma Aldrich, Germany. All aqueous solutions were prepared with distilled and deionized water. All other reagents and chemicals used were of analytical grade.

2.2. Methods

2.2.1. Formulation of curcumin-loaded solid lipid nanoparticles (C-SLNs)

The SLNs were prepared by method previously described by Gupta et al. (2007) with slight modifications. Lipid phase was prepared by melting HSPC:DSPE:Chol:triolein in w/w ratio of 1.5:1:1.2:1 at 80 °C. Curcumin dissolved in ethanol was added to this melt phase at the same temperature. Aqueous phase containing 0.1% (w/v) poloxamer 188 was heated to the same temperature. Melt phase was added to the aqueous phase by rapid injection at 80 °C under high speed homogenization at 25,000 rpm and further homogenized for 15 min. This hot premix was then passed through high pressure homogenizer (GEA Nero Soavi Dynamic) at 800 bar pressure for 10 cycles at 80 °C. After homogenization the suspension was immediately cooled to 4–8 °C and stored. The formed nanoparticle suspension was then filtered through 0.2 μm polyethersulfone membrane filter. The solid lipid nanoparticles were separated by ultracentrifugation at 25,000 × *g* for 30 min at 4 °C. The pellets were resuspended in distilled water and lyophilized in tabletop lyophilizer (LyoPro 3000, Heto-Holten A/S, Allerod, Denmark) for 24 h using mannitol as a cryoprotectant.

2.2.2. Preparation of transferrin conjugated C-SLNs (Tf-C-SLNs)

Tf was covalently coupled by its carboxyl group to the amino group of DSPE present on the surface of preformed curcumin-loaded SLNs using EDC as the coupling agent. The conjugation of transferrin was carried out by the method reported previously by Gupta et al. (2007), with slight modifications. Briefly, C-SLNs were suspended in phosphate buffer (pH 7.4) containing Tf (lipid matrix:Tf ratio: 90:10, w/w) and EDC (1.5%, w/v). This mixture was mixed well by vortexing and kept for 2 h at room temperature. Excessive unbound Tf and EDC were removed by centrifugation using Avanti J-301 centrifuge (Beckman Coulter, USA) at 25,000 × *g* for 10 min and determined by UV spectrophotometry.

2.2.3. Preparation of curcumin solubilized surfactant solution (CSSS)

Curcumin was dissolved in an aqueous system containing 0.1% (w/v) poloxamer 188 by stirring for 15 min at 400 rpm. Aqueous system containing 0.1% (w/v) poloxamer 188 without curcumin was prepared as a blank system and termed as surfactant solution (SS).

2.2.4. Characterization of SLNs

2.2.4.1. Optimization of preparation of SLNs. The composition and processing conditions were finalized after preliminary studies followed by a 3^2 factorial design. The weight ratio of lipids and amount of stabilizer were taken as independent variables and particle size, zeta potential and percent drug entrapment (PDE) were taken as dependent variables. The data has not been included here.

2.2.4.2. Tf conjugation efficiency. The quantitation of Tf conjugation at the surface of the C-SLNs was done by the Bradford assay using coomassie blue G (Bradford, 1976). In brief, the unbound Tf was separated by centrifugation using Avanti J-301 centrifuge (Beckman Coulter, USA) at 25,000 × *g* for 10 min. The pellets were resuspended in 1 ml PBS, mixed with 1 ml Coomassie blue G dye solution and placed in a volumetric flask. Volume was adjusted to 10 ml with distilled water and kept for 30 min at room temperature. The absorbance of Tf was measured at 595 nm using UV–vis spectrophotometer (V-530, Jasco, Japan) and compared with a blank containing the same amount of dye. Conjugation efficiency is expressed as mg of Tf per mM of phospholipids.

2.2.4.3. Physical characterization. The particle size of C-SLNs and Tf-C-SLNs was determined by dynamic light scattering using Malvern Hydro 2000 SM particle size analyzer (Malvern instruments, UK). SLN suspension was added to the sample dispersion unit with stirrer, and stirred so as to minimize the particulate aggregation by interparticle interaction. For the measurement the laser obscuration range was maintained between 2% and 5% (Page-Clisson et al., 1998). The analysis was performed thrice and average hydrodynamic particle size was expressed as the value of *z*-average

size ± S.D. The uniformity of the size distribution was indicated by the polydispersity index (PdI). For morphological characterization and also particle size determination of SLNs, transmission electron microscopy (TEM) was done using Hitachi S-7500 transmission electron microscope (Hitachi, Japan). The SLNs were dispersed in water and one drop of the diluted dispersion was placed on a 200-mesh carbon coated copper grid. The photographs were taken at 30,000× magnification and 100 kV voltage (Mulik et al., 2009). The zeta (ζ) potential was measured by Laser Doppler Velocimetry (Zetasizer 3000, Malvern Instruments, Malvern, UK) at 25 °C. Values are presented as mean ± S.D. from three replicate samples (Mulik et al., 2009). The percentage drug entrapment (PDE) of curcumin in SLNs was determined using the ultracentrifugation method (Beckmann TL-100, MN, USA) (Fry et al., 1978). In brief, the SLNs were centrifuged at 18,000 × *g* for 30 min to obtain pellets of nanoparticles. The supernatant was decanted and pellets were lysed using minimum quantity of ethanol to extract curcumin. This was further diluted with PBS 7.4 and analyzed for drug content using UV–vis spectrophotometer (V-530, Jasco, Japan) at λ_{max} 424 nm. The stability of curcumin in CSSS and SLNs was studied for 6 months at 40 °C/75% relative humidity in the presence and absence of light by determining the drug content using HPLC method using UV–vis detector as previously reported by our group (Mulik et al., 2009). An HPLC apparatus with Borwin/HSS 2000 software (LG 1580-04, JASCO, Japan) equipped with a Vydac, reversed phase C-18 column (250 mm × 4.6 mm, 5 μm, Flexit Jour Lab. Pvt. Ltd., Pune, India) and a UV–vis detector (UV-1575, JASCO, Japan) was used. 0.1% (v/v) trifluroacetic acid (TFA) and acetonitrile (1:1, v/v) (adjusted to pH 3.0 with an ammonia) was used as mobile phase. C-SLNs and CSSS (0.1 ml each) was dissolved in 1 ml acetonitrile separately and centrifuged at 18,000 × *g* for 60 min using ultracentrifuge (Beckmann TL-100, MN, USA). The supernatant was collected and injected into the column. The amount of curcumin was calculated from the peak areas using a calibration curve constructed of standard curcumin. A flow rate of 1.5 ml/min and detection wavelength of 420 were employed. Also, particle size and zeta potential of SLNs was studied over a period of 6 months.

2.2.4.4. X-ray diffraction (XRD) analysis of nanoparticles. X-ray diffraction measurements were carried out with X-ray diffractometer (PW 1729, Philips, Netherlands) in the diffraction range of 5–50°. A Cu-Ka radiation source was used, and the scanning rate (2θ/min) was 5 °C/min. The SLN suspensions were analyzed after vacuum freeze drying (Lee et al., 2007; Jenning et al., 2000).

2.2.4.5. In vitro drug release study. The release pattern of curcumin from C-SLNs was studied using closed double jacketed thermostatic chamber at 37 ± 2 °C using cellophane dialysis bag (cut-off 5000, HiMedia, India) in phosphate buffer as a dialyzing medium (with 50% (v/v) ethanol to maintain the sink condition) under continuous stirring (Tiyaboonchaia et al., 2007). 5 ml each of SLN dispersion with 0.1% (w/v) Tween 80 (as a stabilizer) was placed in two dialysis bags, sealed at both ends which act as a donor compartment. The dialysis bags were then dipped into two different receptor compartments containing 50 ml receptor medium maintained under continuous stirring. At regular time intervals aliquots were withdrawn and replenishment of receptor compartment with same volume of fresh dialyzing medium was done. Analysis was carried out in triplicate using UV–vis spectrophotometer (V-530, Jasco, Japan) and the average values were calculated ($n = 3$). Results were expressed as % cumulative drug release versus time.

2.2.5. Cell culture study

MCF-7 cells were obtained from American Type Culture Collection (ATCC, Manassas, VA) and were grown in RPMI 1640 supplemented with 10% fetal bovine serum and 1% penicillin G-streptomycin (Gibco BRL, Grand Island, NY) at 37 °C in a humidified, 5% CO_2 atmosphere.

2.2.5.1. MTT assay. MCF-7 cells (2×10^4/well) were seeded in a 96-well plate and allowed to attach for 24 h. Then the medium was replaced with fresh medium and the cells were treated with different concentrations of CSSS, C-SLN and Tf-C-SLN (1, 3, 9, 27, 81 μM curcumin/well) using SS and B-SLN as the respective controls and incubated for 24 h at 37 °C in CO_2 incubator. After the treatment, medium was removed, cells were washed three times with PBS and fresh medium was added. Then, 25 μl of 3-(4,5-dimethylthiazol-2-yl)-2,5-diphenyl tetrazolium bromide (MTT) (5 mg/ml in PBS) was added to the cells and incubated for 3 h at 37 °C in CO_2 incubator. MTT gets reduced to purple formazan in living cells by mitochondrial reductase. This reduction takes place only when reductase enzymes are active, and therefore this conversion is used as a measure of viable (living) cells. Then, the cells were lysed and the dark blue crystals were solubilized with 125 μl of a lysis solution (50% (v/v) N,N, dimethylformamide, 20% (w/v) sodium dodecylsulphate, with an adjusted pH of 4.5). The optical density of each well was measured with a Victor 1420 Multilabel Counter (PerkinElmer Life Sci., USA) equipped with a 570 nm filter. Percent of cell survival was defined as the relative absorbance of treated cells versus respective controls. Results were expressed as % cell viability versus dose.

To confirm the Tf-receptor mediated uptake of Tf-C-SLNs, Tf receptors on cell surface were blocked by incubating the cells with an excess amount of free Tf for 1 h prior to incubation with Tf-C-SLNs in a separate experiment and the effect on cell viability was determined after 24 h treatment (Sahoo and Labhasetwar, 2005). For this experiment 3 μM dose of curcumin was used.

The effect of time of treatment on the cell viability was assessed using the same method. In brief, the cells (1×10^5/well) were seeded in 24-well plate and allowed to attach for 24 h. Then, the medium was replaced with fresh medium and treated with CSSS, C-SLN and Tf-C-SLN (5 μM curcumin/well) using SS and B-SLNs as the respective controls and incubated at 37 °C in CO_2 incubator for 3, 6, 12, 24 and 48 h and the effect on cell viability was determined as described above. Results were expressed as % cell viability versus time.

2.2.5.2. Cell uptake study. Both qualitative and quantitative determination of curcumin uptake by MCF-7 cells treated with CSSS, C-SLN, Tf-C-SLN was done using fluorescence microscopy (Weir et al., 2007) and spectrophotometry (Kunwar et al., 2008). For quantitative determination of curcumin uptake by cells, the cells were treated as described above (10 μM curcumin/well) for different time intervals (3, 6, 12, 24, 48 h). At each time point, the cells were washed thrice with PBS 7.4, collected by trypsinization and centrifuged for 3 min at 3000 rpm. The supernatant was decanted and the pellets were resuspended in 1 ml of methanol and vortexed for 5 min to extract the curcumin in methanol fraction. Then, the lysate was centrifuged at 5000 rpm for 5 min and the absorbance of supernatant containing methanolic curcumin was measured at 428 nm using UV–vis spectrophotometer (V-530, Jasco, Japan). From the calibration plot of methanolic curcumin at 428 nm, the amount of curcumin loading into the cells was determined (Kunwar et al., 2008). The effect on Tf-receptor blocking on cell uptake of Tf-C-SLN was also observed after 24 h treatment with 10 μM dose of curcumin. The uptake of curcumin was expressed as μg of curcumin per 10^5 cells.

For qualitative estimation of uptake of curcumin by cells, the autofluorescence of curcumin was observed using fluorescence microscopy using green filter. Cells (1×10^5/well) were seeded in 24-well plate and allowed to attach for 24 h. By replacing the medium with fresh medium, cells were treated with CSSS, C-SLN

and Tf-C-SLN (20 μM curcumin/well) for different time points (6, 12, 24 and 48 h). After each time point, the medium was replaced with fresh medium by washing the cells thrice with PBS 7.4 and the fluorescence images of curcumin were captured using Nikon Eclipse TE300 fluorescence microscope with Nikon F601 camera (Nikon, Japan).

2.2.5.3. Measurement of reactive oxygen species (ROS). The formation of reactive oxygen species was evaluated by means of the probe 2′,7′-dichlorodihydrofluorescein diacetate (H2DCF-DA) method as per previously described (Wang and Joseph, 1999). Briefly, MCF-7 cells (2×10^4/well) were seeded into 96-well plate and allowed to attach for 24 h. Then, the medium was replaced with fresh medium and treated with different concentrations of CSSS, C-SLN and Tf-C-SLN (1, 3, 9, 27, 81 μM curcumin/well) using SS and B-SLNs as the respective controls and incubated for 24 h at 37 °C in CO_2 incubator. After treatment, the medium was removed and the cells were washed thrice with PBS 7.4. 2′,7′-Dichlorodihydrofluorescein diacetate was then added at a final concentration of 10 μM and incubated for 1 h at 37 °C. H2DCF-DA is a non-fluorescent permeant molecule that passively diffuses into cells, where it gets converted to H2DCF as acetates get cleaved by intracellular esterases, and gets entrapped within the cell. In the presence of intracellular ROS, H2DCF get rapidly oxidized to the highly fluorescent 2′,7′-dichlorofluorescein (DCF). Thus, after 2 h incubation, fluorescence was monitored at an excitation wavelength of 502 nm and an emission wavelength of 520 nm using Envision 2104 Multilabel Reader (PerkinElmer Life Sci., USA). Results were expressed as Relative Fluorescence Units (RFU) versus dose.

To confirm the Tf-receptor mediated uptake of Tf-C-SLNs, Tf receptors on cell surface were blocked by incubating the cells with an excess amount of free Tf for 1 h prior to incubation with Tf-C-SLNs in a separate experiment and the effect on ROS generation was determined after 24 h treatment (Sahoo and Labhasetwar, 2005). For this experiment 3 μM dose of curcumin was used.

The effect of time of treatment on the generation of ROS was determined using the same method. In brief, the cells (1×10^5/well) were seeded in 48-well plate and allowed to attach for 24 h. Then, the medium was replaced with fresh medium and treated with CSSS, C-SLN and Tf-C-SLN (5 μM curcumin/well) using SS and B-SLNs as the respective controls and incubated at 37 °C in CO_2 incubator for 3, 6, 12, 24 and 48 h and the generation of ROS at different time points was determined by following the method as described above. Results were expressed as Relative Fluorescence Unit versus time.

2.2.5.4. Cell death analysis. Phosphatidylserine (PS) is exposed during early apoptosis by flipping from the inner to the outer plasma membrane leaflet, and AnnexinV-FITC has the ability to bind to PS with high affinity. Furthermore, propidium iodide (PI) conjugates to necrotic cells (Van et al., 1998; Ganta and Amiji, 2009). On the basis of these phenomena, the double staining with AnnexinV-FITC and PI to detect apoptotic and necrotic cells was performed. MCF-7 cells (1×10^6/flask) were seeded in Nunc cell culture flask (75 cm^2) and allowed to attach for 24 h. Then, after replacing the medium with fresh medium, cells were treated with CSSS, C-SLN and Tf-C-SLN (5 and 10 μM curcumin/well) using SS, B-SLN and free Tf + Tf-C-SLN as the respective controls and incubated for 24 h at 37 °C in CO_2 incubator. After the treatment, medium was removed, cells were detached using trypsin–EDTA solution and suspended in fresh medium. Then, the cells were centrifuged at 3000 rpm for 5 min. Cell pellets were resuspended in AnnexinV binding buffer and centrifugation was repeated again. Finally, the cell pellets were resuspended in AnnexinV binding buffer (1×10^6/ml). 100 μl of this cell suspension was transferred to 5 ml FACS tube, stained with AnnexinV-FITC (5 μl) and 10 μl PI for and incubated for 15 min in dark at room temperature. Finally, 400 μl of AnnexinV binding buffer was added. At this step, treated unstained cells (1×10^6/ml) were also prepared in the same manner, to detect the possible autofluorescence of curcumin in green (FL1) channel. Cells were analyzed by using the flow cytometer (FACSCantoII, BD Biosciences) in FL1 and FL2 channel for FITC and PI, respectively. Green (FITC) fluorescence (FL1) was collected at 535 nm, and red (PI) fluorescence (FL2) at more than 550 nm, from 10,000 cells. The time course study was also carried out using the same procedure for 12, 24 and 48 h time points with 5 μM dose. The result of dose dependent study is expressed as dot plot of AnnexinV-FITC versus PI with quadrant gating. Four distinct cell populations were clearly distinguishable: viable (lower left quadrant, AnnexinV-$FITC^-PI^-$), early apoptotic (lower right quadrant, AnnexinV-$FITC^+PI^-$), late apoptotic and early necrotic (upper right quadrant, AnnexinV-$FITC^+PI^+$), and late necrotic (upper left quadrant, AnnexinV-$FITC^-PI^+$). The result of time dependent study is expressed as bar chart indicating the respective percentages of early apoptotic, and late apoptotic and early necrotic. The % of cells was determined by using FACSDiva software.

2.2.5.5. Cell cycle analysis. Cell cycle analysis is an important parameter for the detection of cells undergoing apoptosis (Weir et al., 2007; Shi et al., 2006). Cell phase distribution was assayed by the determination of DNA contents. To determine the effect of CSSS, C-SLN and Tf-C-SLN on the cell cycle, treated cells were analyzed using a flow cytometer. In brief, cells (1×10^6/flask) were seeded in Nunc cell culture flask (75 cm^2) and allowed to attach for 24 h. Then, the cells were treated with CSSS, C-SLN and Tf-C-SLN (5 and 10 μM curcumin/well) using SS, B-SLN and free Tf + Tf-C-SLN as the respective controls and incubated for 24 h at 37 °C in CO_2 incubator. After the treatment, cells were harvested by centrifugation, washed with PBS and fixed in 70% ethanol for 2 h. The cells were then centrifuged to remove ethanol, washed and resuspended in 500 μl PBS 7.4 containing RNase (100 μg/ml) at room temperature for 30 min. Then, the cellular DNA was stained with PI (50 μg/ml) and kept in dark for 30 min to stain DNA. The cell cycle was analyzed by a flow cytometer [FACSCantoII flow cytometer (BD 409 Biosciences)] in red (FL2) channel at more than 550 nm, from 10,000 cells. The % of subG1 fraction was determined by using FACSDiva software.

2.2.5.6. Detection of mitochondrial membrane potential loss ($\Delta\Psi_m$). Loss of mitochondrial membrane potential ($\Delta\Psi_m$), indicative of late stage of apoptosis, was detected using lipophilic, cationic fluorescent redistribution dye tetramethylrhodamine methyl (TMRM) ester (Skommer et al., 2006). Briefly, MCF-7 cells (1×10^6/flask) were cultured and allowed to attach for 24 h. Then, the cells were treated with CSSS, C-SLN and Tf-C-SLN (5 and 10 μM curcumin/well) using SS, B-SLN and free Tf + Tf-C-SLN as the respective controls and incubated for 24 h at 37 °C in CO_2 incubator. After the treatment, medium was removed, cells were detached using trypsin–EDTA solution and suspended in fresh medium. Then, the cells were centrifuged at 3000 rpm for 5 min and pellets were resuspended in PBS 7.4. 500 μl of this cell suspension was transferred to 5 ml FACS tube, stained with 100 nM TMRM and kept for incubation at 37 °C for 20 min in dark. Further, 500 μl of PBS was added after incubation and the intensities of red fluorescence of 10,000 cells were analyzed by flow cytometer [FACSCantoII flow cytometer (BD 409 Biosciences)] in FL2 channel at more than 550 nm. The % of these low $\Delta\Psi_m$ cells was determined by using FACSDiva software.

2.2.6. Statistical analysis

All the experiments were performed in triplicate and results were expressed as mean ± S.D. ($n = 3$). Statistical analysis was done

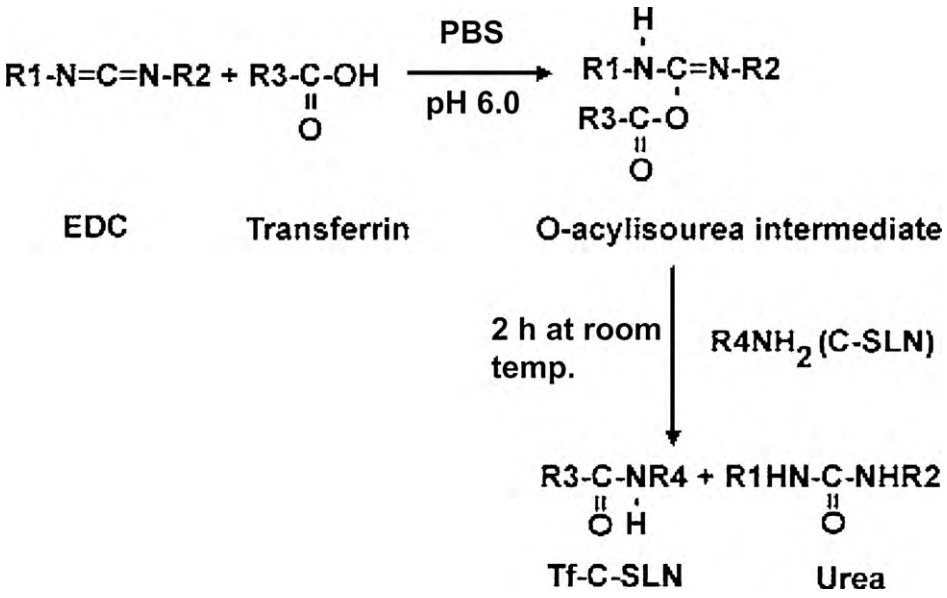

Fig. 1. Schematic representation of transferrin conjugation with C-SLNs. C-SLNs: curcumin-loaded solid lipid nanoparticles; DSPE: distearoyl phosphatidylethanolamine; and EDC: 1-ethyl-3-[3-dimethylaminopropyl]carbodiimide hydrochloride.

by performing Student's *t* test. The differences were considered significant for p values of <0.05.

3. Results

From the factorial design study, based on the results of particle size, zeta potential and PDE of all nine batches, the optimized batch was determined. This optimized batch was used for the further study.

3.1. Tf conjugation and conjugation efficiency

In Tf conjugation experiment with SLNs, Tf was first mixed with EDC in suitable proportions in PBS 7.4. At this step, carboxyl group of Tf reacts with EDC to form an amine reactive *O*-acylisourea intermediate. This intermediate then reacts with amine group of DSPE on the surface of SLNs after the addition of Tf-EDC mixture to the SLN suspension to form stable amide bond between Tf and SLNs and an EDC by-product is released as a soluble urea derivative (DeSilva, 2003; Grabarek and Gergely, 1990) (Fig. 1). This conjugation of Tf with SLNs was quantitated by Bradford assay. The conjugation efficiency was found to be 21.59 mg Tf per mM phospholipids. It was found that the method was highly efficient for the conjugation of Tf by quantifying the actual amount of Tf conjugated on the surface of SLNs.

3.2. Physical characterization of SLNs

The mean particle size of C-SLN was found to be 194 ± 2.89 nm with a polydispersity index of 0.15. There was no significant change in particle size after Tf conjugation. The particle size of Tf-C-SLN was found to be 206 ± 3.2 nm with a polydispersity index of 0.18. Also, the spherical nature and particle size of SLNs was confirmed by TEM study (Fig. 2). The ζ potential of C-SLNs was 12.43 ± 1.58 mV which shifts towards more negative side after conjugation of Tf to the SLNs. The ζ potential of Tf-C-SLN was 8.21 ± 0.89 mV. The PDE of C-SLNs was determined by ultracentrifugation and it was found to be $77.27 \pm 2.34\%$ indicating good encapsulation efficiency of the prepared SLNs. The stability study showed increased stability of curcumin against photodecomposition in SLNs compared to CSSS. The percentage curcumin remained in the absence and presence of light after 3 and 6 months in C-SLNs was significantly more compared to that in CSSS (Table 1). There was no significant difference in the particle size and zeta potential of C-SLNs after 6 months indicating the good physical stability of the prepared SLNs (data not shown). These results of particle size, ζ potential, PDE and stability

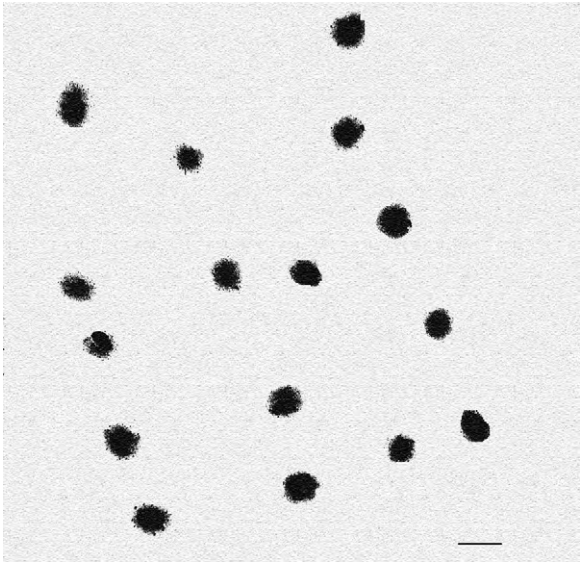

Fig. 2. Transmission electron microscopy of curcumin-loaded solid lipid nanoparticles (C-SLNs). The magnification bar in the image is 200 nm.

Table 1
Stability study of curcumin.

Condition	%Curcumin remaining in CSSS (% ± S.D. $n = 3$)	%Curcumin remaining in C-SLNs (% ± S.D. $n = 3$)
40 °C/75% RH in absence of sunlight		
3 Months	62 ± 1.8	89 ± 2.3
6 Months	55.6 ± 3.1	82.7 ± 2.9
40 °C/75% RH in presence of sunlight		
3 Months	54.8 ± 2.3	84.3 ± 2.7
6 Months	49.8 ± 3.2	78.7 ± 2.6

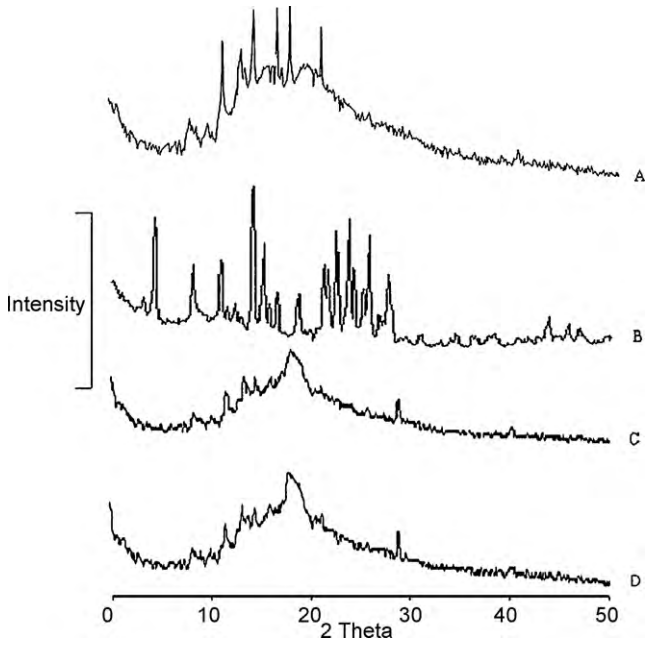

Fig. 3. X-ray diffraction (XRD) patterns. Sample A: bulk matrix, Sample B: curcumin solubilized surfactant solution (CSSS), Sample C: blank SLNs (B-SLNs), and Sample D: curcumin-loaded solid lipid nanoparticles (C-SLNs).

showed good efficiency of the method of preparation used for the formulation of SLNs and their stable nature.

3.3. XRD analysis of SLNs

The diffraction pattern of the curcumin, blank SLN (B-SLN) and C-SLN was analyzed (Fig. 3). From the diffraction patterns of both B-SLN and C-SLN, it was clear that less ordered crystals were majority, and thus, the amorphous state would contribute to the higher drug loading capacity. The diffraction pattern of curcumin showed remarkable difference from those of C-SLNs. The sharp peaks of curcumin, indicating the crystalline nature, were not present in the diffraction pattern of C-SLNs indicating that curcumin is entrapped in the lipid core of SLNs and that too in amorphous or molecular dispersion form. Also, looking at the diffraction patterns of B-SLN and C-SLN, there was not much difference in the pattern, indicating that the addition of curcumin has not changed the nature of SLNs. An explanation to this observation is that the curcumin is entrapped in the lipid core of SLNs. X-ray diffraction patterns of the B-SLN and C-SLN were broader and much weaker than that of the bulk matrix. It indicated that lipid matrix in the SLNs was less ordered or loosely arranged. One more important observation was that both B-SLN and C-SLN showed characteristic peak at 19.62°, which is an indicator of typical βi polymorph and lower crystallinity index value (Lee et al., 2007). This result corroborate with some reports (Lee et al., 2007; Jenning et al., 2000) which states that in the preparation of SLNs, lipids can be arranged in the more thermodynamically stable β or βi polymorph rather than the α polymorphic form.

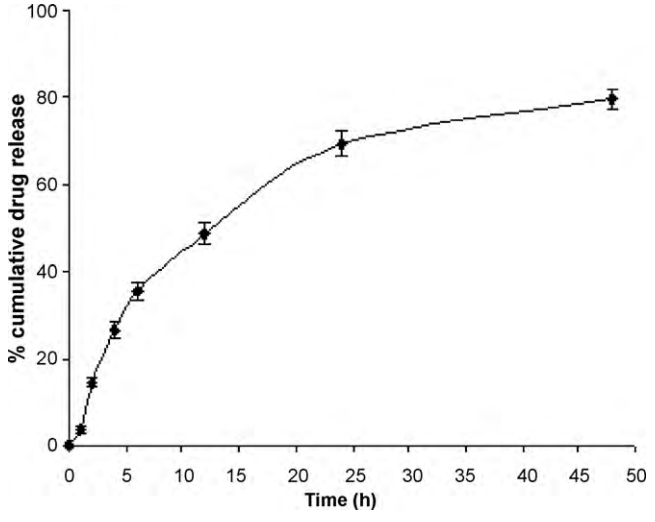

Fig. 4. *In vitro* release profile of curcumin from curcumin-loaded solid lipid nanoparticles (C-SLNs). Each point represents the mean value ± S.D. ($n = 3$).

3.4. In vitro drug release study

In this study, since curcumin is water insoluble, 50% (v/v) ethanol was used in the receptor medium (Tiyaboonchaia et al., 2007). *In vitro* release study showed initial burst release for the first 5–6 h which can be attributed to the adsorbed drug on the surface of SLNs. After 12 h, the release pattern was more steady indicating the sustained drug release from SLNs. The percentage cumulative drug release after 48 h was 84.3 ± 4.1% (Fig. 4). The release pattern

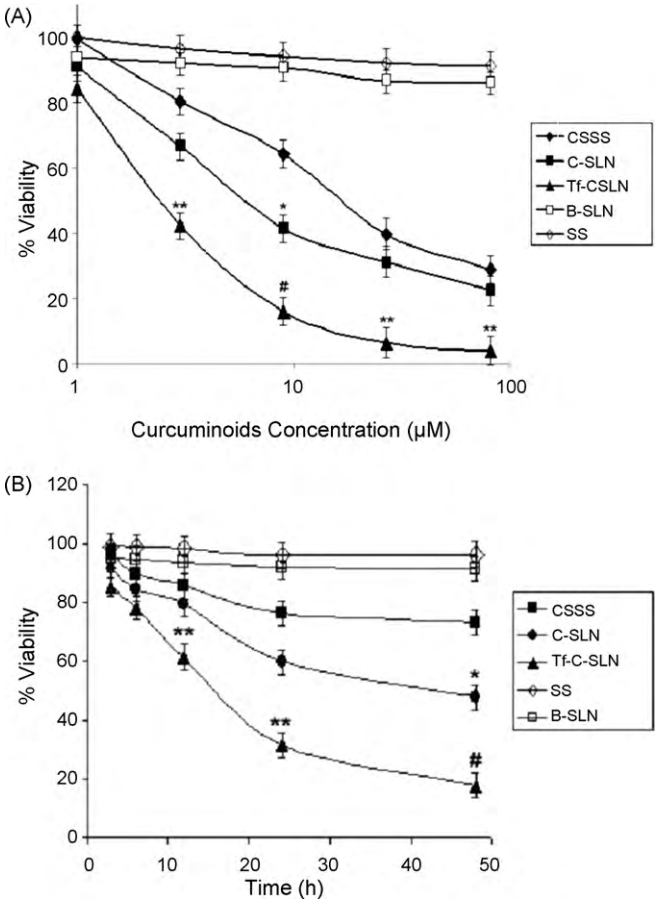

Fig. 5. Antiproliferative activity study. (A) Dose dependent cytotoxicity: MCF-7 cells were treated with different concentrations of CSSS, C-SLNs, Tf-C-SLNs, SS, and B-SLNs. The extent of growth inhibition was measured after 24 h by performing MTT assay. Data is represented as mean ± S.D. ($n = 3$). (**) $p < 0.05$, Tf-C-SLNs versus CSSS and C-SLN, (*) $p < 0.05$, C-SLN versus CSSS, (#) $p < 0.005$, Tf-C-SLN versus CSSS. (B) Time dependent cytotoxicity: MCF-7 cells were treated with 5 μM dose of CSSS, C-SLNs, Tf-C-SLNs, SS, and B-SLNs. The extent of growth inhibition was measured after predetermined time points of 3, 6, 12, 24, 48 h by performing MTT assay. Data is represented as mean ± S.D. ($n = 3$). (**) $p < 0.05$, Tf-C-SLNs versus CSSS and C-SLN, (*) $p < 0.05$, C-SLN versus CSSS, (#) $p < 0.005$, Tf-C-SLN versus CSSS and C-SLN. CSSS: curcumin solubilized surfactant solution; C-SLNs: curcumin-loaded solid lipid nanoparticles; Tf-C-SLNs: Tf-conjugated curcumin-loaded solid lipid nanoparticles; SS: surfactant solution; and B-SLNs: blank SLNs.

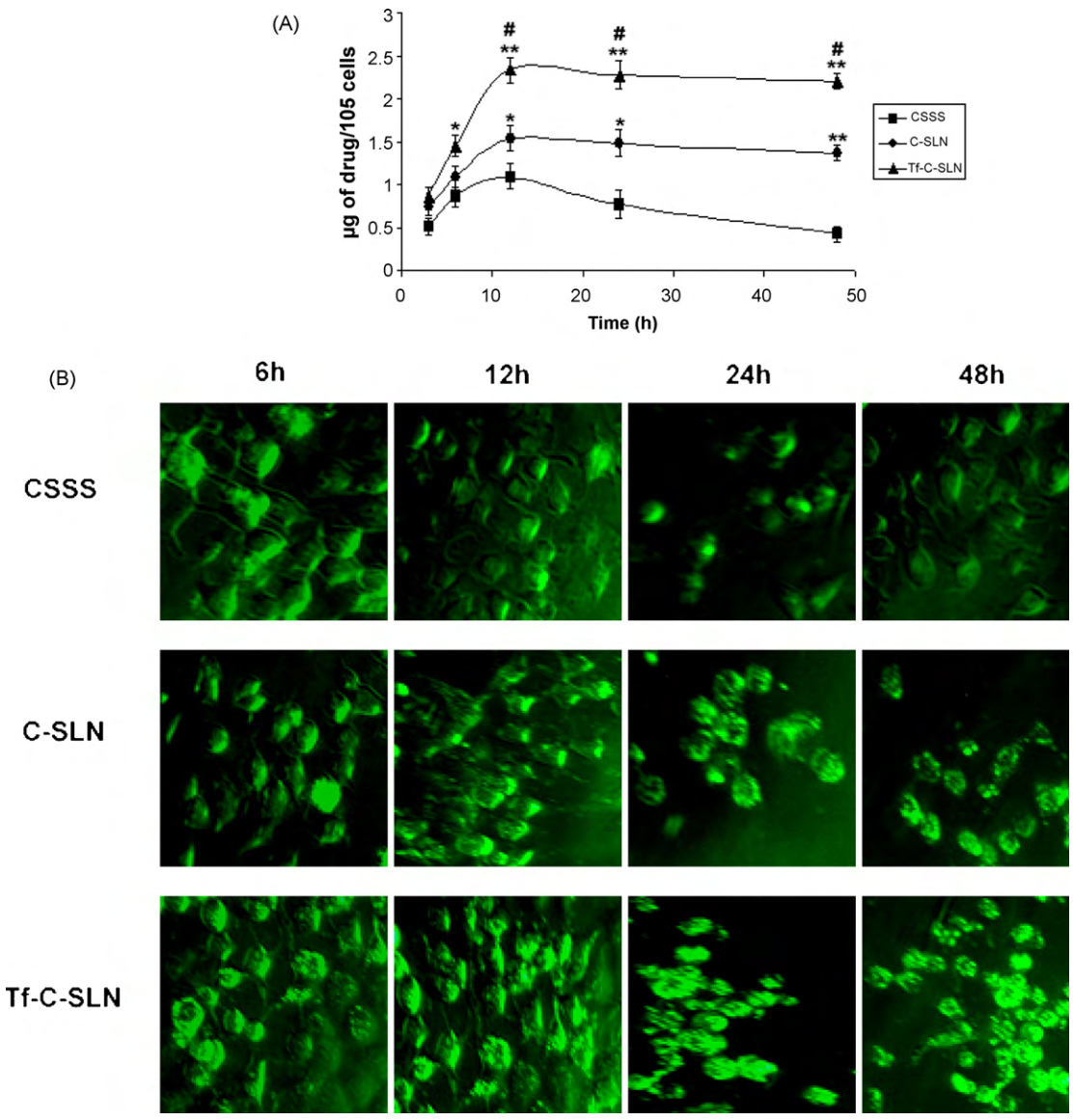

Fig. 6. (A) Quantitative intracellular uptake of curcumin from CSSS, C-SLNs, Tf-C-SLNs by MCF-7 cell line at 37 °C. Cells were treated with 10 μM dose. Data as mean ± S.D. ($n = 3$). (*) $p < 0.05$, Tf-C-SLNs or C-SLNs versus CSSS, (**) $p < 0.005$, Tf-C-SLNs or C-SLNs versus CSSS, (#) $p < 0.05$, Tf-C-SLNs versus C-SLNs. (B) Fluorescence microscopy images showcasing the time dependent (6, 12, 24 and 48 h) intracellular uptake of curcumin from CSSS, C-SLNs, Tf-C-SLNs (20 μM curcumin) by MCF-7 cells. CSSS: curcumin solubilized surfactant solution; C-SLNs: curcumin-loaded solid lipid nanoparticles; and Tf-C-SLNs: Tf-conjugated curcumin-loaded solid lipid nanoparticles.

of Tf-C-SLNs was also studied and it was observed that there was no considerable difference in release behavior compared to C-SLNs. Tf-C-SLNs showed slightly slower release compared to C-SLNs which may be because Tf conjugation creates double barrier effect for the diffusion of the drug (data not shown) (Gupta et al., 2007).

3.5. Cell culture study

3.5.1. Antiproliferative activity

The effect of increase in curcumin concentration on the antiproliferative action was assessed by MTT assay. It was observed that with CSSS, C-SLN and Tf-C-SLN, the antiproliferative activity increased dose dependently (Fig. 5A). At the lowest dose (1 μM), no significant difference in activity was observed in three formulations. However, at the concentrations above 3 μM, significant difference was observed in cell viability between three formulations. At 3 μM dose, the cell viability was 80.3 ± 2.1% and 66.7 ± 2.4%, respectively, for CSSS and C-SLN. At the same dose, cell viability was reduced to 42.4 ± 1.78% with Tf-C-SLN showing stronger effect than the other formulations studied. At 9 μM dose, the effect was even more pronounced. The cell viability was reduced to 64.2 ± 1.2% with CSSS, while the cell viability with C-SLN was reduced more significantly to 41.3 ± 1.3% showing the significant reduction in cell viability compared to CSSS. The cell viability was reduced to 14.5 ± 0.7% with Tf-C-SLN, showing again the higher potency than the other formulations. Further, increase in dose to 27 μM showed significant reduction in viability with CSSS, but, there was not much significant reduction with C-SLN and Tf-C-SLN. Still, there was significant difference between Tf-C-SLN and CSSS, C-SLN. At the highest dose of 81 μM, the effect was almost similar with CSSS and C-SLN reducing the cell viability to 28.91 ± 1.21% and 22.45 ± 1.44%, respectively, while the cell viability was 4.01% with Tf-C-SLN at this dose (Fig. 5A).

In a separate experiment of Tf-receptor blocking, it was observed that excessive addition of free Tf with Tf-C-SLN significantly affected the antiproliferative activity of Tf-C-SLN. The cell viability after 24 h treatment with Tf-C-SLN was 42.42 ± 1.89%, compared to 85.67 ± 1.33% with Tf-C-SLN + free Tf, showing the

reduced antiproliferative effect of Tf-C-SLN because of Tf-receptor blocking on cell surface.

The effect of treatment time on the antiproliferative activity of CSSS, C-SLN and Tf-C-SLN was also studied using 5 μM curcumin concentration (Fig. 5B). It was observed that there was not much difference in the cell viability after 3 and 6 h treatment with three formulations. However, at later time points, Tf-C-SLN reduced the cell viability considerably more than CSSS and C-SLN. There was no significant difference in the effect between CSSS and C-SLN until 24 h treatment, but at 48 h, C-SLN was significantly more effective than CSSS indicating the sustained release effect of SLNs (Fig. 5B). In both dose and time dependent study, SS and B-SLN were taken as respective controls for CSSS, C-SLN and Tf-C-SLN. Since, these controls showed negligible effect on cell viability (Fig. 5A and B), the antiproliferative effect observed with all the three formulations was confirmed to be because of curcumin.

3.5.2. Cell uptake study

The quantitative estimation of curcumin uptake by MCF-7 cells from all three formulations showed prominent difference in curcumin levels (Fig. 6A). In all three treatment groups, highest drug levels were observed at 12 h treatment. The drug levels in CSSS, C-SLN and Tf-C-SLN treated cells after 12 h were 1.09 ± 0.11, 1.54 ± 0.14 and 2.3 ± 0.12 μg per 10^5 cells, respectively. After 24 h treatment, the drug levels reduced to 0.77 ± 0.09, 1.48 ± 0.11 and 2.28 ± 0.13 μg per 10^5 cells in CSSS, C-SLN and Tf-C-SLN, respectively. At the end of the experiment (48 h), the reduction in drug levels of CSSS treated cells was more significant (0.43 ± 0.069 μg per 10^5 cells) compared to C-SLN treated cells (1.37 ± 0.11 μg per 10^5 cells) and Tf-C-SLN treated cells (2.21 ± 0.15 μg per 10^5 cells). In an experiment of Tf-receptor blocking, the drug levels from Tf-C-SLN were significantly lower in blocked cells (0.8 ± 0.1 μg per 10^5 cells) compared to unblocked cells (2.28 ± 0.13 μg per 10^5 cells).

The fluorescence microscopy study for the qualitative determination of cell uptake of curcumin from CSSS, C-SLN and Tf-C-SLN formulations revealed that the cell uptake from C-SLN and Tf-C-SLN was more sustained compared to CSSS (Fig. 6B). In CSSS treated cells, the fluorescence intensity was good after 6 and 12 h but it was reduced with time. After 24 and 48 h, the fluorescence intensity reduced significantly. In case of C-SLN and Tf-C-SLN treated cells, the fluorescence intensity increased after 6 h and it remained almost steady even after 48 h, suggesting the sustained intracellular release and retention of encapsulated curcumin from SLNs localized inside the cells. The fluorescence intensity of Tf-C-SLN treated cells was more after 24 and 48 h compared to C-SLN treated cells suggesting receptor mediated endocytosis. At all time points, the fluorescence intensity of C-SLN and Tf-C-SLN was more compared to CSSS. Images of untreated cells were also taken to see possible autofluorescence. No autofluorescence was observed in untreated control cells.

3.5.3. Measurement of ROS generation

The generation of ROS was measured with different concentrations of curcumin in CSSS, C-SLN and Tf-C-SLN. The results were expressed as RFU of fluorescent DCF and an increase in RFU indicates increased ROS generation. With all three formulations, curcumin increased RFU dose dependently. Tf-C-SLN induced higher ROS compared to CSSS and C-SLN at the doses above 3 μM (Fig. 7A). C-SLN also seemed to induce ROS generation more than CSSS, but this difference was significant only at the 9 μM concentration.

In a separate experiment of Tf-receptor blocking, it was observed that excessive addition of free Tf with Tf-C-SLN significantly affected the ROS generation of Tf-C-SLN. The ROS generation with Tf-C-SLN was significantly reduced with preaddition of free Tf compared to Tf-C-SLN alone indicating the effect of Tf-receptor

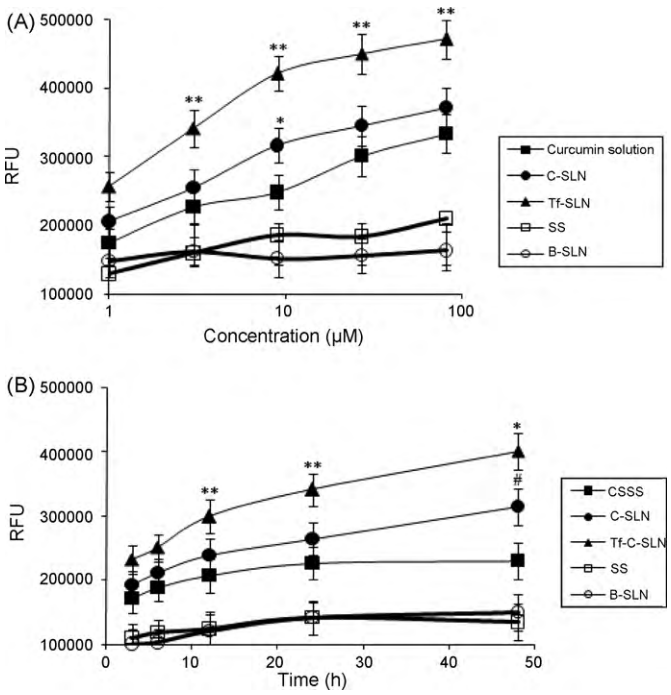

Fig. 7. (A) Effect of dose on generation of reactive oxygen species (ROS) by CSSS, C-SLNs, Tf-C-SLNs, SS and B-SLN in MCF-7 cells after 24 h treatment was determined by ROS assay using H2DCF-DA. Data as mean ± S.D. ($n = 3$). (**) $p < 0.05$, Tf-C-SLNs versus CSSS and C-SLNs, (*) $p < 0.05$, C-SLNs versus CSSS. (B) Effect of time of treatment on generation of ROS by CSSS, C-SLNs, Tf-C-SLNs, SS and B-SLN. MCF-7 cells were treated with three formulations (5 μM curcumin) and generation of ROS was determined at predetermined time points of 3, 6, 12, 24 and 48 h. Data as mean ± S.D. ($n = 3$). (**) $p < 0.05$, Tf-C-SLNs versus CSSS and C-SLNs, (*) $p < 0.005$, Tf-C-SLNs versus CSSS, (#) $p < 0.05$ C-SLNs versus CSSS. CSSS: curcumin solubilized surfactant solution; C-SLNs: curcumin-loaded solid lipid nanoparticles; Tf-C-SLNs: Tf-conjugated curcumin-loaded solid lipid nanoparticles; SS: surfactant solution; and B-SLNs: blank SLNs.

blocking on the cell surface and hence, reduced uptake of Tf-C-SLN in the presence of free Tf. Hence, the Tf-mediated endocytosis in case of Tf-C-SLN was confirmed.

The effect of time course of treatment on the generation of ROS was also studied with 5 μM curcumin concentration. The increase in ROS generation with time was more pronounced in case of Tf-C-SLN compared to CSSS and C-SLN with significant increase after 12 h (Fig. 7B). C-SLN showed significantly higher ROS generation compared to CSSS only at 24 and 48 h treatment. These results were in agreement with the results of previous study of time dependent antiproliferative activity and cell uptake study. The controls used in both dose and time dependent study (SS and B-SLNs) showed negligible effect on ROS generation (Fig. 5A and B) indicating the ROS generation observed with all the three formulations was indeed because of curcumin.

3.5.4. Determination of phosphatidylserine externalization

Externalization of PS at the outer plasma membrane is an early event in apoptosis which is a consequence of loss of plasma membrane asymmetry Hence, this PS externalization was detected as an indicator of apoptosis by targeting for the loss of plasma membrane asymmetry by method described earlier (Van et al., 1998). The induction of apoptosis by curcumin after the treatment with all three formulations was detected and quantified by flow cytometry (Fig. 8A). Initially, the possible autofluorescence of curcumin was checked using treated unstained cells. The signal obtained at used concentrations (5 and 10 μM) was very weak. Hence, it was confirmed that curcumin is not interfering in the study (Skommer et al., 2006). The apoptotic cells were observed in cells treated with

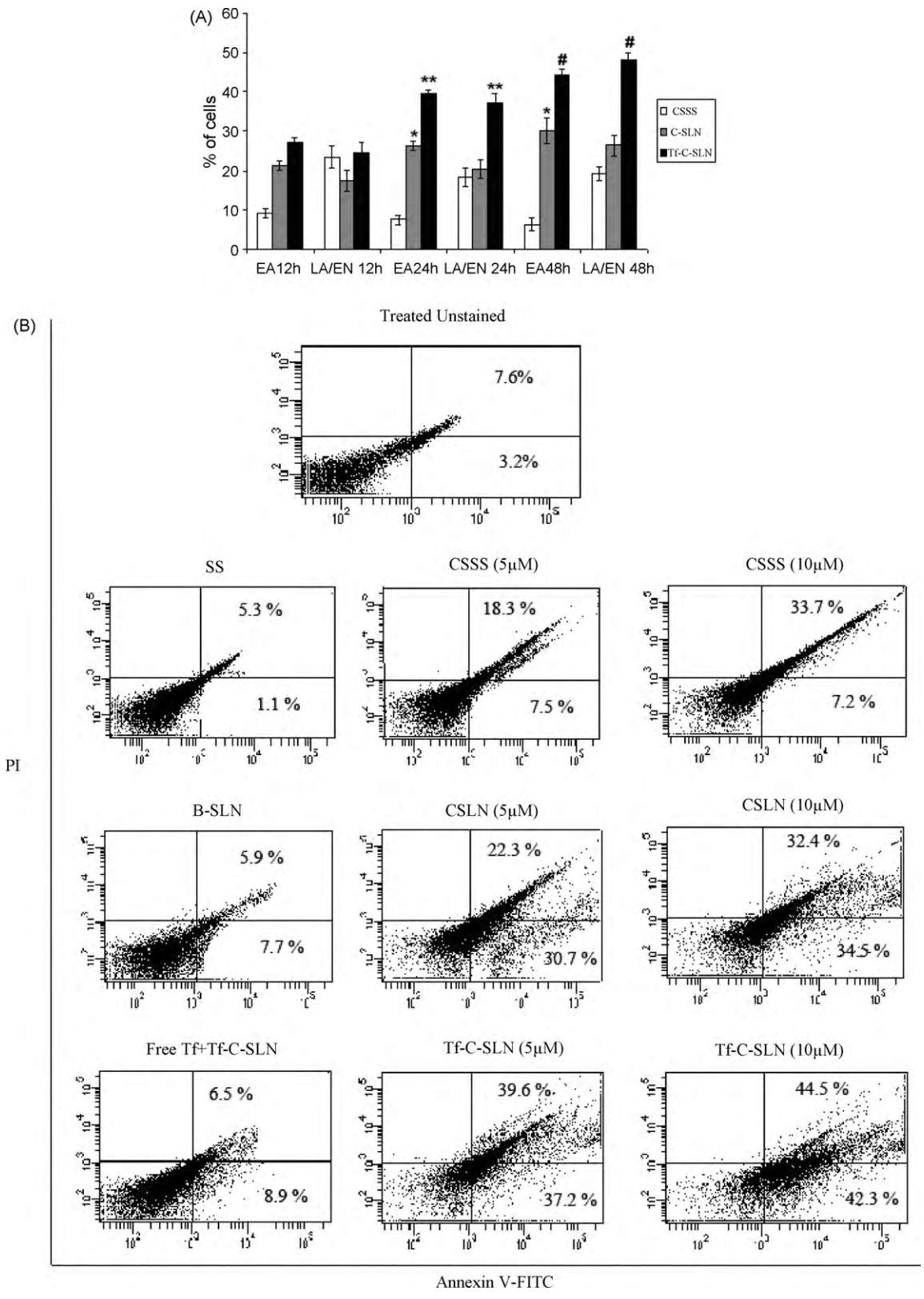

Fig. 8. Quantitative apoptotic measurement in MCF-7 cells after treatment with CSSS, C-SLNs, Tf-C-SLNs, SS, B-SLNs and free Tf + Tf-C-SLNs. (A) Dose dependent effect on apoptosis by treatment with 5 and 10 μM dose for 24 h was determined by flow cytometry analysis. Results of dose dependent effect are expressed as dot plot of AnnexinV-FITC versus PI and representative values from three experiments are shown. Dot plot from flow cytometry analysis reveals the four different populations of cells. Top left: necrotic cells (AnnexinV-FITC$^-$PI$^+$); top right: late apoptotic cells (AnnexinV-FITC$^+$PI$^+$); bottom left: live cells (AnnexinV-FITC$^-$PI$^-$); and bottom right: early apoptotic cells (AnnexinV-FITC$^+$PI$^-$). Statistically significant effect was observed when apoptotic activity of Tf-C-SLNs was compared with that of CSSS and C-SLN and C-SLNs compared with CSSS at $p < 0.05$. (B) Effect of time of treatment on apoptotic activity at predetermined time points 12, 24 and 48 h with 5 μM dose was determined by flow cytometry. The results are expressed as bar chart. Data as mean ± S.D. ($n = 3$) (**) $p < 0.05$, Tf-C-SLNs versus CSSS and C-SLN, (*) $p < 0.05$, C-SLN versus CSSS, (#) $p < 0.005$, Tf-C-SLN versus CSSS and C-SLN. EA: early apoptotic; LA: late apoptotic; and EN: early necrotic.

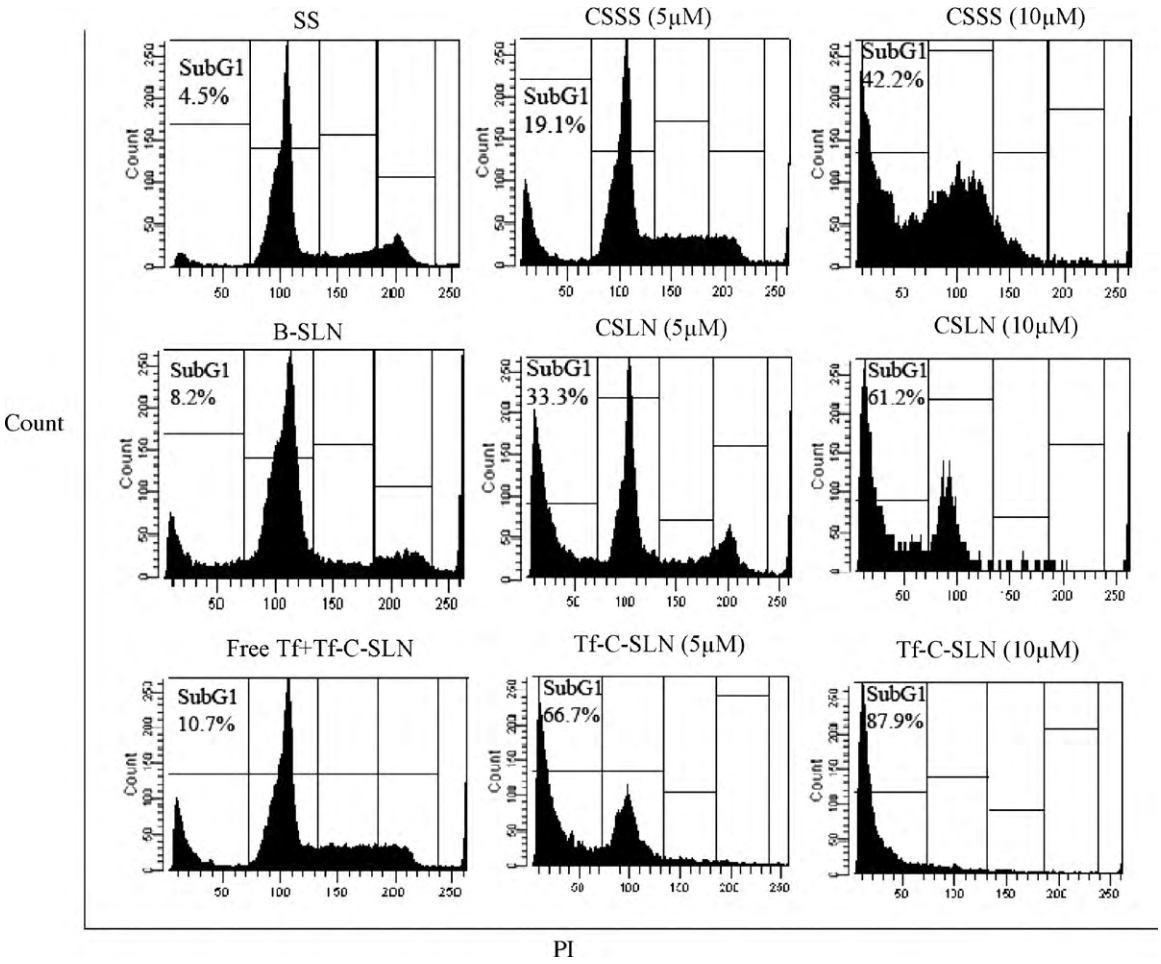

Fig. 9. Effect of CSSS, C-SLNs, Tf-C-SLNs, SS, B-SLNs, and free Tf + Tf-C-SLNs on cell cycle analysis was determined by flow cytometry with 5 and 10 μM dose. The increase in subG1 fraction was monitored and the representative values of three experiments are shown. The histogram plot represents the distribution of cells in subG1, G0/G1, S and G2/M phase.

all the three formulations but the percentage of apoptotic cells varied with each formulation. Tf-C-SLN treated cells showed 37.2% and 39.6% of early apoptotic (AnnexinV-FITC$^+$PI$^-$) and late apoptotic/early necrotic (AnnexinV-FITC$^+$PI$^+$) populations, respectively, compared to CSSS (7.5% and 18.3%) and C-SLN (30.7% and 22.3%) treated cells at 5 μM dose for 24 h. At the higher concentration of 10 μM, an increase in both populations was observed with all three formulations. The percentage of early apoptotic (AnnexinV-FITC$^+$PI$^-$) and late apoptotic/early necrotic (AnnexinV-FITC$^+$PI$^+$) populations in cells treated with CSSS, C-SLN and Tf-C-SLN at 10 μM dose were 5.7% and 33.7%, 34.5% and 32.4%, 42.3% and 44.5%, respectively.

In a separate experiment, the effect of the treatment time on apoptosis induction was also studied with 12, 24 and 48 h time points using 5 μM curcumin concentration (Fig. 8B). Tf-C-SLN treated cells showed 27.2% and 24.5%, 39.6% and 37.2% of early apoptotic (AnnexinV-FITC$^+$PI$^-$) and late apoptotic/early necrotic (AnnexinV-FITC$^+$PI$^+$) populations, respectively, compared to CSSS (9.1% and 23.4%, 7.5% and 18.3%) and C-SLN (22.3% and 17.4%, 26.3% and 20.4%) treated cells at 12 and 24 h, respectively. With longer treatment time (48 h), an increase in both the populations was observed significantly in C-SLN and Tf-C-SLN treated cells compared to CSSS treated cells. The percentage of early apoptotic (AnnexinV-FITC$^+$PI$^-$) and late apoptotic/early necrotic (AnnexinV-FITC$^+$PI$^+$) populations in cells treated with CSSS, C-SLN and Tf-C-SLN after 48 h were 6.2% and 19.1%, 30.2% and 26.4%, 44.3% and 48.2%, respectively. Experiment with controls (SS, B-SLN) showed that they have negligible apoptotic effect indicating the apoptosis induced by all the formulations was indeed because of curcumin. It was clearly evident from the results of Tf-receptor blocking experiment that the blocking significantly reduced the apoptotic effect of Tf-C-SLNs confirming the role of Tf-receptor mediated endocytosis in enhanced apoptotic activity of Tf-C-SLNs.

3.5.5. Cell cycle analysis

Cell cycle damage is one of the important feature for the detection of apoptotic cells. Hence, the cell cycle analysis was carried out to determine the fraction of DNA content in subG1 level which is an indicator of apoptosis. The effect of dose was studied with all the three formulations and the percentage of subG1 fraction was determined by FACSDiva software (Fig. 9). Again, Tf-C-SLN treated cells showed significantly more % of DNA content in subG1 phase compared to CSSS and C-SLN treated cells. At 5 μM dose, the subG1 fraction in CSSS, C-SLN and Tf-C-SLN treated cells were 19.1%, 33.3% and 66.7%, respectively, which increased to 42.2%, 61.2% and 87.9%, respectively, at 10 μM dose. Hence, it was confirmed that Tf-C-SLNs were more efficient in apoptosis induction compared to CSSS and C-SLN. SS, B-SLN showed negligible effect indicating the non-toxic nature of controls used. Also, the Tf-receptor blocking experiment confirmed that the enhanced apoptotic effect of Tf-C-SLNs was because of increased uptake of Tf-C-SLNs by Tf-receptor mediated endocytosis.

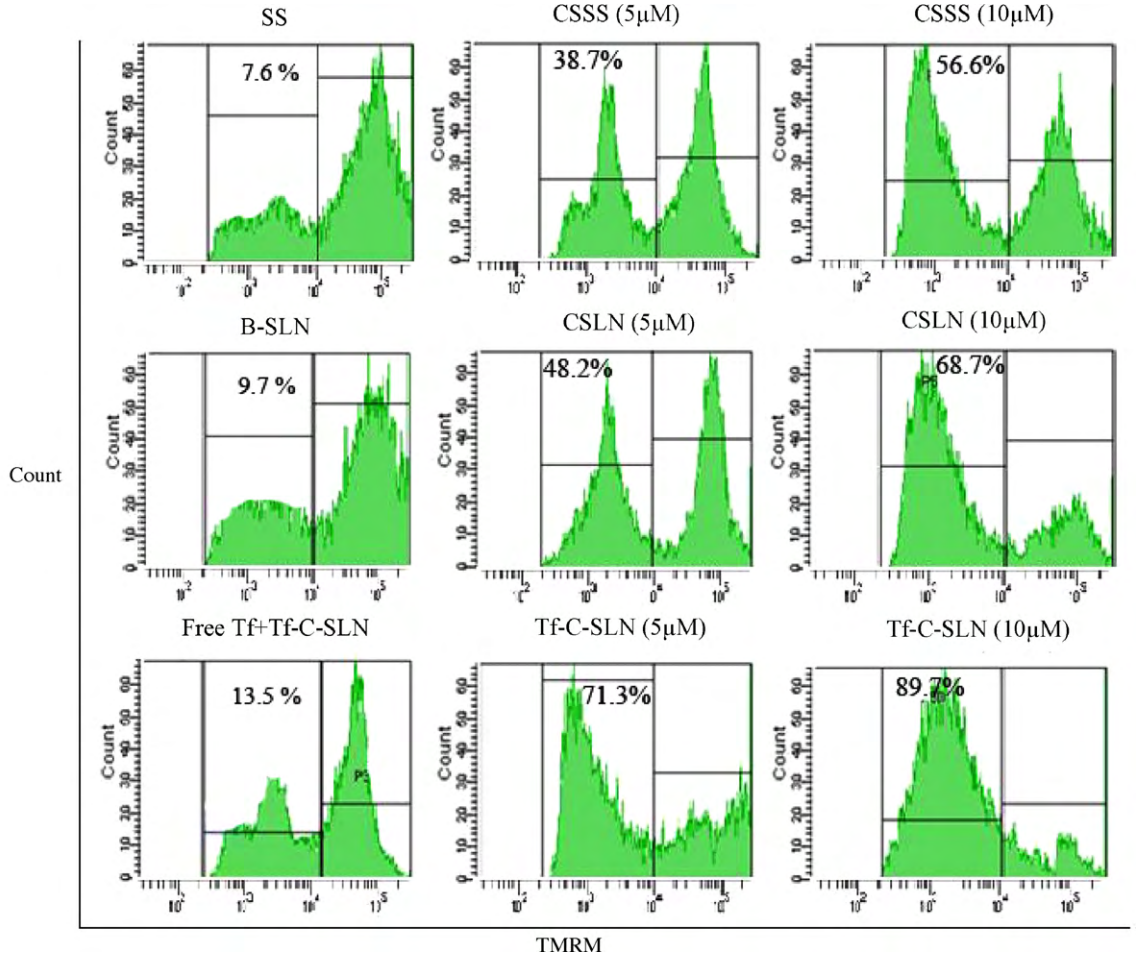

Fig. 10. Determination of decrease in mitochondrial membrane potential in MCF-7 cells after treatment with 5 and 10 μM dose of CSSS, C-SLNs, Tf-C-SLNs, SS, B-SLNs, and free Tf+Tf-C-SLNs was done by flow cytometry using TMRM staining. The shift of TMRM positive signal (viable/high MMP cells) to TMRM negative signal (apoptotic/low MMP cells) was monitored and the representative values of apoptotic/low MMP cells from three experiments are shown. The results are expressed as histogram of flow cytometry analysis.

3.5.6. Detection of mitochondrial membrane potential loss ($\Delta\Psi_m$)

TMRM staining was used for the detection of $\Delta\Psi_m$. TMRM accumulates in the mitochondria in proportion to membrane potential. Thus, viable cells with proper $\Delta\Psi_m$, accumulates TMRM in the mitochondria and hence, TMRM positive cells (high $\Delta\Psi_m$ cells) is an indication of viable cells. On the other hand, in apoptotic cells because of reduced $\Delta\Psi_m$, TMRM releases from the mitochondria and hence, TMRM negative cells (low $\Delta\Psi_m$ cells) indicate mitochondria mediated apoptosis. From the histogram of flow cytometry analysis, it was observed that cells treated with all the three formulations showed TMRM negative signals (low $\Delta\Psi_m$ cells) indicating the presence of apoptotic cells (Fig. 10). At 5 μM dose, the percentage of low $\Delta\Psi_m$ cells in CSSS, C-SLN and Tf-C-SLN treated cells was 38.7%, 48.2% and 71.3%, respectively, which increased to 56.6%, 68.7% and 89.7%, respectively, at 10 μM dose. Tf-C-SLN treated cells showed more percentage of low $\Delta\Psi_m$ cells compared to CSSS and C-SLN treated cells with both doses. Both the controls (SS, B-SLN) showed negligible effect on MMP indicating their non-toxic nature. Further, Tf-mediated endocytosis of Tf-C-SLN was confirmed from the receptor blocking experiment.

4. Discussion

Therapeutic potential of curcumin as an anticancer agent is very well documented (Anand et al., 2008; Chattopadhyay et al., 2004). However, the therapeutic efficacy of curcumin always gets hampered by some of its drawbacks. First, its oral bioavailability is very low (Anand et al., 2007) and, hence, the oral administration of curcumin is not feasible. Another important drawback of curcumin is its photodecomposition (Ansari et al., 2005; Acharya et al., 2009). So, there is a need to develop drug delivery system capable of preventing these drawbacks. There are numerous reports on therapeutic potential of curcumin and/or curcuminoids as an anticancer agent using cell culture studies, but, certain questions still remain unanswered. In all these reports, curcumin and/or curcuminoids are used in solution form using organic solvents like DMSO, ethanol, methanol (Ramachandran et al., 2002; Aggarwal et al., 2005a,b) and some with aqueous solutions (Kunwar et al., 2008) making curcumin very vulnerable to photodegradation. The use of organic solvents is also not recommended for *in vivo* use. There is only one report on enhanced antiproliferative activity using Tf-mediated nanoparticles containing paclitaxel in MCF-7 cells (Sahoo and Labhasetwar, 2005). However, there are no reports on Tf-mediated drug delivery systems containing curcumin till date. Hence, considering all these factors, in the present study, we propose transferrin mediated solid lipid nanoparticulate formulation of curcumin capable of overcoming the abovementioned drawbacks. The fate of any drug delivery system after *in vivo* administration mainly depend on its physicochemical properties, hence physicochemical characterization of prepared nanoparticles is very significant. Since, particle size and zeta potential affects physical

stability, biodistribution and release pattern of nanoparticles and also its cellular uptake, it is an important parameter of evaluation. The determination of encapsulation of curcumin inside the prepared nanoparticles is important from the stability and release point of view. The encapsulation of curcumin inside the SLNs was confirmed by XRD study. It was observed that curcumin was encapsulated in an amorphous or molecularly dispersed form (Lee et al., 2007). Thus, being encapsulated inside the nanoparticles its photodegradation can be prevented and we can get sustained drug release. From *in vitro* release study it was observed that SLNs sustained the release of curcumin for 48 h. The antiproliferative activity of all the three formulations was studied using the MTT assay both in dose and time dependent manner. It was observed that Tf-C-SLN has significantly more antiproliferative activity at lower dose of 3 and 9 μM compared to CSSS and C-SLN suggesting the effect of increased intracellular uptake of Tf-C-SLNs by Tf-receptor mediated endocytosis.

In time course study, C-SLN and Tf-C-SLN showed prominent effect of time of treatment on their antiproliferative activity compared to CSSS. This result can be attributed to the sustained release effect (and hence increased retention time) of SLNs in the intracellular region corroborating the *in vitro* release data. Tf-C-SLN showed more noticeable difference in antiproliferative activity after 12 h compared to CSSS and C-SLN. The increased antiproliferative activity of Tf-C-SLN in both dose and time dependent study was in agreement with the hypothesis proposed by Sahoo and Labhasetwar (2005). According to this hypothesis, Tf-conjugated delivery systems could have different intracellular sorting pathway after uptake by Tf-receptor mediated endocytosis compared to unconjugated delivery systems via nonspecific pathway and this could increase the intracellular retention and hence, therapeutic efficacy of the encapsulated drug molecule.

In a separate experiment, the effect of Tf-receptor blocking on the performance of Tf-C-SLN was observed to confirm the Tf-mediated endocytosis of Tf-C-SLN. It was observed from this experiment that Tf-receptor blocking significantly reduced the activity of Tf-C-SLN. The antiproliferative activity of Tf-C-SLN was reduced by 1.5 fold in Tf-receptor blocked cells compared to unblocked cells confirming the uptake of Tf-C-SLN by MCF-7 cells was indeed because of Tf-receptor mediated endocytosis (Sahoo and Labhasetwar, 2005).

The cellular uptake of curcumin from all the three formulations was studied both qualitatively and quantitatively by fluorescence microscopy and UV spectroscopy. The effect of time of treatment on cellular uptake of curcumin from all the three formulations was studied qualitatively by fluorescence microscopy. It was clear from the fluorescence intensity of intracellular curcumin that the uptake was more from Tf-C-SLN compared to CSSS and C-SLN. Also, the reduction in fluorescence intensity with time in CSSS treated cells suggests the possible efflux of curcumin with time and noncapability of sustained release (Ganta and Amiji, 2009). On the other hand, both C-SLN and Tf-C-SLN showed increase in fluorescence intensity compared to CSSS and even after 48 h treatment prominent fluorescence intensity was observed with SLNs. These observations were an indication of sustained release of curcumin from both SLNs compared to CSSS. Also the increased fluorescence intensity in Tf-C-SLN treated cells compared to C-SLN treated cells further affirms the agreement with the hypothesis of increased drug uptake and retention proposed by Sahoo and Labhasetwar (2005).

In quantitative estimation of cell uptake, maximum drug levels were obtained at 12 h treatment. After that, the drug levels were reduced significantly in CSSS treated cells compared to C-SLN and Tf-C-SLN treated cells. At 12 h, Tf-C-SLN and C-SLN treated cells showed about 2.5 and 1.5 fold increase in drug uptake compared to CSSS treated cells. The increase in drug levels of Tf-C-SLN and C-SLN treated cells after 24 h treatment was about 4 and 2 fold, respectively, compared to CSSS treated cells which further increased to >5 and >3 fold, respectively, after 48 h treatment. Tf-C-SLNs treated cells showed about 2 fold increase in drug levels at all time points compared to C-SLN treated cells. Thus, Tf-C-SLN treated cells showed higher drug uptake at all time points compared to CSSS and C-SLN treated cells. These results were further corroborating the results of previous studies and proposed mechanisms of increased cell uptake, sustained drug release and increased drug retention. The effect of Tf-receptor blocking on the uptake of Tf-C-SLN was observed. In case of blocked cells the uptake of curcumin from Tf-C-SLN was significantly reduced supporting the proposed Tf-receptor mediated endocytosis of Tf-C-SLNs.

Curcumin is known to induce apoptosis by increasing the generation of ROS (Buttke and Sandstrom, 1994; Jacobson, 1996; Christine et al., 2004). Thus, we studied the effect of all the three formulations on generation of ROS in dose and time dependent manner. At all doses above 3 μM, it was observed that Tf-C-SLN treated cells showed >3 and >1.5 fold increase in ROS generation compared to CSSS and C-SLN treated cells. In time course study, the ROS generation was increased with time in C-SLN and Tf-C-SLN treated cells while in CSSS treated cells the ROS generation almost became stagnant after 12 h substantiating the results of cell uptake.

As the time dependent study was carried out with lower dose of 5 μM, it was observed that even with lower dose, Tf-C-SLN showed prominent increase in ROS generation with increase in time of treatment. These results were confirmatory for the previous observations obtained with antiproliferative activity and cell uptake study attributing the increased generation of ROS with C-SLN and Tf-C-SLN to the sustained release of encapsulated curcumin from both SLNs, increased uptake of Tf-C-SLN by Tf-receptor mediated endocytosis and increased retention.

Apoptosis study also showed the increased therapeutic potential of Tf-C-SLNs compared to CSSS and C-SLNs as more apoptosis was detected in Tf-C-SLN treated cells compared to CSSS and C-SLN treated cells. The increase in cell death with Tf-C-SLNs was about 3 and 1.5 fold more compared to CSSS and C-SLN while C-SLN showed 2 fold increase in cell death compared to CSSS. In time dependent study, Tf-C-SLN treated cells showed almost 90% apoptosis at the end of 48 h treatment, indicating the enhanced activity with Tf-C-SLN even at the low dose of 5 μM compared to CSSS and C-SLN ($\leq$30% and $\leq$60%, respectively). The effect of time of treatment on apoptosis was more prominent with C-SLN and Tf-C-SLN compared to CSSS. With C-SLN and Tf-C-SLN treated cells almost 1.5 fold increase in cell death was observed after 48 h compared to 24 h. This result can be attributed to the sustained release of curcumin from intracellular SLNs over longer period of time (Sahoo and Labhasetwar, 2005).

One important observation from both the dose and time dependent apoptosis study was detection of distinctly more late apoptotic/early necrotic cells (AnnexinV-FITC$^+$PI$^+$) than early apoptotic cells (AnnexinV-FITC$^+$PI$^-$) in CSSS treated cells which can be attributed to the diffusion and accumulation of curcumin at high concentration directly at the site of action causing more necrosis. In C-SLN and Tf-C-SLN treated cells early apoptotic (AnnexinV-FITC$^+$PI$^-$) cells were almost similar or slightly less compared to late apoptotic/early necrotic cells (AnnexinV-FITC$^+$PI$^+$) in dose dependent study suggesting the slow progression from early apoptotic to late apoptotic/early necrotic population because of slow and sustained release of curcumin.

In cell cycle analysis, the presence of hypodiploid peak in subG1 region is an indication of apoptosis (Weir et al., 2007). Hence, the % of subG1 fraction was determined and compared with all the three formulations. Tf-C-SLN treated cells showed almost 2–3 fold increase in subG1 fraction compared to CSSS treated cells while, 1.5–2 fold increase compared to C-SLN treated cells. This result was

in accordance with the previous results suggesting the increased uptake and retention with Tf-C-SLN by proposed mechanisms.

The loss of mitochondrial membrane potential is one of the end-point features of apoptosis (Skommer et al., 2006). In this $\Delta\Psi_m$ measurement study, Tf-C-SLN treated cells showed more percentage of low $\Delta\Psi_m$ cells compared to CSSS and C-SLN treated cells with both doses as expected from the previous results. Hence, determination of low $\Delta\Psi_m$ cells further confirmed the increased therapeutic efficacy of curcumin with Tf-C-SLN.

Thus, Tf-conjugated drug delivery system increased the intracellular uptake of curcumin. But, increased uptake is not the only reason for increased therapeutic efficacy but increased intracellular retention compared to unconjugated systems and solution forms also play an important part (Sahoo and Labhasetwar, 2005). The most probable reason for this effect is different cellular uptake mechanisms of these systems. Cellular uptake of Tf-conjugated system is by Tf-receptor mediated endocytosis while unconjugated system enters the cell via nonspecific endocytosis and drug in solution form enters by passive diffusion. This difference may be influencing the distribution and retention of the drug intracellularly. From our study, we demonstrated that Tf-C-SLNs showed enhanced anticancer activity in both dose and time dependent study compared to CSSS and C-SLNs supporting the abovementioned mechanism. Hence, from our study we propose that developed Tf-conjugated drug delivery system is better therapeutic drug delivery system for curcumin in the treatment of breast cancer.

5. Conclusion

From the present study, we conclude that proposed drug delivery system of curcumin is suitable for the effective delivery of curcumin considering the aspects of sustained release, biocompatible and biodegradable nature, and the targeting effect. The increased efficacy of curcumin against MCF-7 breast cancer cells using targeting effect of Tf-C-SLNs confirmed the potential of proposed drug delivery in the treatment of breast cancer. Based on the results from present study, the proposed transferrin mediated drug delivery system can be used for other types of cancers like brain, prostate, etc.

Acknowledgements

We are very thankful to Centre for International Mobility (CIMO), Helsinki, Finland for providing the Sitra Fellowship (Grant No. 1.10.2008/TM-08-5817/Sitra Fellowship) Also, authors would like to thank Mr. Markku Taskinen, senior laboratory technician, University of Kuopio for his technical help in the study.

Disclosure: The authors have no other relevant affiliations or financial involvement with any organization or entity with a financial interest in or financial conflict with the subject matter or materials discussed in the manuscript apart from those disclosed. No writing assistance was utilized in the production of this manuscript.

References

Acharya, S., Dilnawaz, F., Sahoo, S.K., 2009. Targeted epidermal growth factor receptor nanoparticle bioconjugates for breast cancer therapy. Biomaterials, doi:10.1016/j.biomaterials.2009.07.008.

Aggarwal, B.B., Harikumar, K.B., 2009. Potential therapeutic effects of curcumin, the anti-inflammatory agent, against neurodegenerative, cardiovascular, pulmonary, metabolic, autoimmune, and neoplastic diseases. Int. J. Biochem. Cell Biol. 41, 40–59.

Aggarwal, B.B., Kumar, A., Aggarwal, M.S., Shishodia, S., 2005a. Curcumin derived from turmeric (*Curcuma longa*): a spice for all seasons. In: Phytopharmaceuticals in Cancer Chemoprevention. CRC Press LLC, pp. 349–387.

Aggarwal, B.B., Kumar, A., Bharti, A., 2003a. Anticancer potential of curcumin: preclinical and clinical studies. Anticancer Res. 23, 363–398.

Aggarwal, B.B., Shishodia, S., Takada, Y., 2005b. Curcumin suppresses the paclitaxel-induced nuclear factor-{kappa}B pathway in breast cancer cells and inhibits lung metastasis of human breast cancer in nude mice. Clin. Cancer Res. 11, 7490–7498.

Aggarwal, B., Swaroop, P., Protiva, P., Raj, S.V., Shirin, H., Holt, P.R., 2003b. Cox-2 is needed but not sufficient for apoptosis induced by Cox-selective inhibitors in colon cancer cells. Apoptosis 8, 649–654.

Anand, P., Kunnumakkara, A.B., Newman, R.A., Aggarwal, B.B., 2007. Bioavailability of curcumin: problems and promises. Mol. Pharmacol. 4, 807–818.

Anand, P., Sundaram, C., Jhurani, S., Kunnumakkara, A.B., Aggarwal, B.B., 2008. Curcumin and Cancer: an "old-age" disease with an "age-old" solution. Cancer Lett. 267, 133–164.

Ansari, M.J., Ahmad, S., Kohli, K., Ali, J., Khar, R.K., 2005. Stability indicating HPTLC determination of curcumin in bulk drug and pharmaceutical formulations. J. Pharm. Biomed. Anal. 39, 132–138.

Azuine, M.A., Bhide, S.V., 1992. Chemopreventive effect of turmeric against stomach and skin tumors induced by chemical carcinogens in Swiss mice. Nutr. Cancer 17, 77–83.

Bradford, M.A., 1976. Rapid and sensitive method for the quantitation of microgram quantities of protein utilizing the principle of protein-dye binding. Anal. Biochem. 72, 248–254.

Buttke, T.M., Sandstrom, P.M., 1994. Oxidative stress as a mediator of apoptosis. Immunol. Today 15, 7–10.

Chattopadhyay, I., Biswas, K., Bandyopadhyay, U., Banerjee, R.K., 2004. Turmeric and curcumin: biological actions and medicinal applications. Curr. Sci. 87, 44–53.

Chearwae, W., Wu, C.P., Chu, H.Y., Lee, T.R., Ambudkar, S.V., Limtrakul, P., 2006. Curcuminoids purified from turmeric powder modulate the function of human multidrug resistance protein 1 (ABCC1). Cancer Chemother. Pharmacol. 57, 376–388.

Chearwae, W., Anuchapreeda, S., Nandigama, K., Ambudkar, S.V., Limtrakul, P., 2004. Biochemical mechanism of modulation of human P-glycoprotein (ABCB1) by curcumin I, II, and III purified from Turmeric powder. Biochem. Pharmacol. 68, 2043–2052.

Christine, S.A., Kumari, L., Khar, A., 2004. Effect of curcumin on normal and tumor cells: role of glutathione and bcl-2. Mol. Cancer Ther. 3, 1101–1108.

DeSilva, N.S., 2003. Interactions of surfactant protein D with fatty acids. Am. J. Respir. Cell Mol. Biol. 29, 757–770.

Dorai, T., Cao, Y.C., Dorai, B., Buttyan, R., Katz, A.E., 2001. Therapeutic potential of curcumin in human prostate cancer. III. Curcumin inhibits proliferation, induces apoptosis, and inhibits angiogenesis of LNCaP prostate cancer cells in vivo. Prostate 47, 293–303.

Fry, D.W., White, J.C., Goldman, I.D., 1978. Rapid separation of low molecular weight solutes from liposomes without dilution. J. Anal. Biochem. 90, 803–807.

Ganta, S., Amiji, M., 2009. Coadministration of paclitaxel and Curcumin in nanoemulsion formulations to overcome multidrug resistance in tumor cells. Mol. Pharmacol. 6, 928–939.

Grabarek, Z., Gergely, J., 1990. Zero-length crosslinking procedure with the use of active esters. Anal. Biochem. 185, 131–135.

Gupta, V., Aseh, A., Rios, C.N., Aggarwal, B.B., Mathur, A.B., 2009. Fabrication and characterization of silk fibroin-derived curcumin nanoparticles for cancer therapy. Int. J. Nanomed. 4, 115–122.

Gupta, Y., Jain, A., Jain, S.K., 2007. Transferrin-conjugated solid lipid nanoparticles for enhanced delivery of quinine dihydrochloride to the brain. J. Pharm. Pharmacol. 59, 935–940.

Hussain, N., 2000. Ligand-mediated tissue specific drug delivery. Adv. Drug Deliv. Rev. 43, 95–100.

Jacobson, M.D., 1996. Reactive oxygen species and programmed cell death. Trends Biochem. Sci. 21, 83–86.

Jenning, V., Korting, M.S., Gohla, S., 2000. Vitamin A-loaded solid lipid nanoparticles for topical use: drug release properties. J. Control. Release 66, 115–126.

Joe, B., Vijaykumar, M., Lokesh, B.R., 2004. Biological properties of curcumin-cellular and molecular mechanisms of action. Crit. Rev. Food Sci. Nutr. 44, 97–111.

Kunwar, A., Barik, A., Mishra, B., Rathinasamy, K., Pandey, R., Priyadarsini, K.I., 2008. Quantitative cellular uptake, localization and cytotoxicity of Curcumin in normal and tumor cells. Biochem. Biophys. Acta 1780, 673–679.

Lemieux, P., Page, M., 1994. Sensitivity of multidrug-resistant MCF-7 cells to a transferrin-doxorubicin conjugate. Anticancer Res. 14, 397–403.

Lee, G.S., Lee, D.H., Kang, K.C., Lee, C., Pyo, H.B., Choi, T.B., 2007. Preparation and characterization of bis-ethylhexyloxyphenolmethoxyphenyltriazine (BEMT) loaded solid lipid nanoparticles (SLN). J. Ind. Eng. Chem. 13, 1180–1187.

Li, J.L., Wanga, L., Liu, X.Y., 2009. In vitro cancer cell imaging and therapy using transferrin-conjugated gold nanoparticles. Cancer Lett. 274, 319–326.

Maruyama, K., Ishida, O., Kasaoka, S., 2004. Intracellular targeting of sodium mercaptoundecahydrododecaborate (BSH) to solid tumors by transferrin–PEG liposomes, for boron neutron-capture therapy (BNCT). J. Control. Release 98, 195–207.

Mulik, R., Mahadik, K.R., Paradkar, A.R., 2009. Development of curcuminoids loaded poly(butyl) cyanoacrylate nanoparticles: physicochemical characterization and stability study. Eur. J. Pharm. Sci. 37, 395–404.

Page-Clisson, M.E., Pinto, H.A., Ourevitch, M., Andremont, A., Couvreur, P., 1998. Development of ciprofloxacin-loaded nanoparticles: physicochemical study of the drug carrier. J. Control Release 56, 23–32.

Qian, Z.M., Li, H., Sun, H., Ho, K., 2002. Targeted drug delivery via the transferrin receptor-mediated endocytosis pathway. Pharmacol. Rev. 54, 561–587.

Ramachandran, C., Fonseca, H.B., Jhabvala, P., Escalon, E.A., Melnick, S.J., 2002. Curcumin inhibits telomerase activity through human telomerase reverse transcriptase in MCF-7 breast cancer cell line. Cancer Lett. 184, 1–6.

Sahoo, S.K., Labhasetwar, V., 2005. Enhanced antiproliferative activity of transferrin-conjugated paclitaxel-loaded nanoparticles is mediated via sustained intracellular drug retention. Mol. Pharmacol. 2, 373–383.

Shi, M., Cai, Q., Yao, L., Mao, Y., Ming, Y., Ouyang, G., 2006. Antiproliferation and apoptosis induced by curcumin in human ovarian cancer cells. Cell Biol. Int. 30, 221–226.

Singh, S., Aggarwal, B.B., 1995. Activation of transcription factor NF-kB is suppressed by curcumin (diferulolylmethane). J. Biol. Chem. 270, 24995–25000.

Skommer, J., Wlodkowic, D., Pelkonen, J., 2006. Cellular foundation of curcumin-induced apoptosis in follicular lymphoma cell lines. Exp. Hematol. 34, 463–474.

Thangapazham, R.L., Sharma, A., Maheshwari, R.K., 2006. Multiple molecular targets in cancer chemoprevention by curcumin. AAPS J. 8, E443–E449.

Tiyaboonchaia, W., Tungpradita, W., Plianbangchang, P., 2007. Formulation and characterization of curcuminoids loaded solid lipid nanoparticles. Int. J. Pharm. 337, 299–306.

Ulbrich, K., Hekmatara, T., Herbert, E., Kreuter, J., 2009. Transferrin and transferrin-receptor-antibody-modified nanoparticles enable drug delivery across the blood–brain barrier (BBB). Eur. J. Pharm. Biopharm. 71, 251–256.

Vandewalle, B., Granier, A.M., Peyrat, J.P., Bonneterre, J., Lefebvre, J., 1985. Transferrin receptors in cultured breast cancer cells. J. Cancer Res. Clin. Oncol. 110, 71–76.

Van, E.M., Nieland, L.W., Ramaekers, F.S., Schutte, B., Reutelingsperger, C.M., 1998. Annexin V-affinity assay: a review on an apoptosis detection system based on phosphatidylserine externalization. Cytometry 31, 1–9.

Wang, F., Jiang, X., Yang, D.C., Elliott, R.L., Head, J.F., 2000. Doxorubicin-gallium-transferrin conjugate overcomes multidrug resistance: evidence for drug accumulation in the nucleus of drug resistant MCF-7/ADR cells. Anticancer Res. 20, 799–808.

Wang, H., Joseph, J.A., 1999. Quantifying cellular oxidative stress by dichlorofluorescein assay using microplate reader. Free Radic. Biol. Med. 27, 612–616.

Weir, N.M., Selvendiran, K., Kutala, V.K., 2007. Curcumin induces G2/M arrest and apoptosis in cisplatin-resistant human ovarian cancer cells by modulating Akt and p38 MAPK. Cancer Biol. Ther. 6, 178–184.

Widera, A., Norouziyan, F., Shen, W.C., 2003. Mechanisms of Tfr-mediated transcytosis and sorting in epithelial cells and applications toward drug delivery. Adv. Drug Deliv. Rev. 55, 1439–1466.

Yang, X., Koh, C.G., Liu, S., 2009. Transferrin receptor-targeted lipid nanoparticles for delivery of an antisense oligodeoxyribonucleotide against bcl-2. Mol. Pharmacol. 6, 221–230.